NASA TECHNICAL NOTE

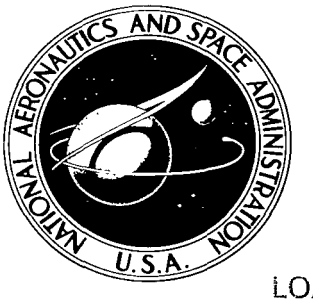

NASA TN D-2047

NASA TN D-2047

EFFECTS OF DIFFERENTIAL PRESSURE, THERMAL STRESS, AND BUCKLING ON FLUTTER OF FLAT PANELS WITH LENGTH-WIDTH RATIO OF 2

by Sidney C. Dixon and Charles P. Shore

Langley Research Center
Langley Station, Hampton, Va.

NATIONAL AERONAUTICS AND SPACE ADMINISTRATION • WASHINGTON, D. C. • DECEMBER 1963

EFFECTS OF DIFFERENTIAL PRESSURE, THERMAL STRESS, AND BUCKLING ON FLUTTER OF FLAT PANELS WITH LENGTH-WIDTH RATIO OF 2

By Sidney C. Dixon and Charles P. Shore

Langley Research Center
Langley Station, Hampton, Va.

NATIONAL AERONAUTICS AND SPACE ADMINISTRATION

EFFECTS OF DIFFERENTIAL PRESSURE, THERMAL STRESS, AND BUCKLING ON FLUTTER OF FLAT PANELS WITH LENGTH-WIDTH RATIO OF 2

By Sidney C. Dixon and Charles P. Shore

SUMMARY

Flat, single-bay, skin-stiffener panels with length-width ratios of 2 were tested at a Mach number of 3.0 and at various dynamic pressures, stagnation temperatures, and differential pressures in order to determine some of the effects of thermal stress, differential pressure, and buckling on the flutter characteristics of elastically restrained panels.

Two distinct flutter boundaries were obtained, one associated with standing-wave flutter and the other with traveling-wave flutter. Standing-wave flutter usually occurred when the differential pressure Δp was less than 0.10 psi; traveling-wave flutter usually occurred when Δp was greater than 0.15 psi and the direction of the loading was toward the cavity behind the panel. The flutter trends indicated by both boundaries were similar to experimental trends obtained previously for thermally stressed panels with length-width ratios from 0.96 to 10. The standing-wave flutter results are compared with theory for the condition of zero midplane stress.

INTRODUCTION

Flutter characteristics of thermally stressed panels have become important with the advent of sustained supersonic flight and the aerodynamic heating associated with such flight conditions. Some effects of compressive stress and buckling, induced by aerodynamic heating, on the flutter characteristics of flat rectangular panels have been reported in references 1 to 5. These investigations revealed that increases in panel skin temperature (or midplane compressive stress in the direction of air flow) makes a flat (unbuckled) panel more susceptible to flutter. The flutter trends are reversed for thermally buckled panels; thus, a panel is most susceptible to flutter when on the verge of buckling. The experimental trends presented in reference 2 for a length-width ratio of 0.96 were similar to the theoretical predictions of references 6 to 10 (for panels subjected to compressive stress only), and the data were in fair numerical agreement for conditions of zero midplane stress and at the onset of buckling. However, for panels with large length-width ratios (where higher mode flutter occurred) large discrepancies existed between theoretical and experimental trends. (See ref. 11.)

Since theoretical methods have not advanced enough to determine reliable panel flutter boundaries, experimental results are generally used in design work. The dearth of available experimental data on the effects of the many parameters affecting the flutter characteristics of panels indicates the need for additional experimental investigations.

The present investigation was conducted in the Langley 9- by 6-foot thermal structures tunnel and was undertaken to determine some effects of compressive stress and buckling (induced by aerodynamic heating) on the flutter characteristics of elastically restrained panels with length-width ratios of 2.0. Single-bay panels, 24 inches long and 12 inches wide, were tested at a Mach number of 3.0 at various dynamic pressures and stagnation temperatures. The differential pressure acting on the panels was controlled manually during the tests. During the initial part of the investigation the differential pressure was not accurately controlled and unusual effects of changes in the pressure difference across the panels were disclosed. Thereafter, this parameter was more precisely controlled in order to investigate these effects.

The flutter data obtained in this investigation are presented in tabular form and also are summarized in terms of nondimensional parameters in the form of flutter boundaries to indicate some effects of differential pressure, midplane compressive stress, and buckling on panel flutter. The experimental data are compared with theoretical results for simply supported and clamped panels for the condition of zero midplane stress.

SYMBOLS

a panel length (longitudinal direction, parallel to air flow)

b panel width (lateral direction, perpendicular to air flow)

D panel flexural stiffness, $\frac{Eh^3}{12(1 - \mu^2)}$

E Young's modulus

f frequency of flutter

h panel skin thickness

M Mach number

$N_x = \sigma_x h$

p_∞ free-stream static pressure

p_b static pressure in cavity behind panel

Δp differential pressure acting on panel skin, $p_b - p_\infty$

q dynamic pressure

T temperature

T_t stagnation temperature

ΔT average increase of panel skin temperature

t time

α coefficient of thermal expansion of panel skin

$\beta = \sqrt{M^2 - 1}$

μ Poisson's ratio (taken equal to 0.3)

σ_x average midplane stress in longitudinal direction

σ_y average midplane stress in lateral direction

TESTS

Panels

The single-bay panels were of skin-stiffener construction and consisted of flat sheets of 0.037-, 0.050-, 0.063-, and 0.078-inch-thick 17-7 PH stainless steel riveted to channel-section stiffeners by single rows of rivets along the longitudinal and lateral edges. The panels were 24 inches long and 12 inches wide (between center lines of rivet rows). The stiffeners were approximately 1.65 inches deep and were formed from 0.078-inch-thick 17-7 PH stainless steel. Pertinent panel construction details are given in figure 1.

Test Apparatus

Tunnel.- All tests were conducted in the Langley 9- by 6-foot thermal structures tunnel, a Mach 3, intermittent blowdown facility exhausting to the atmosphere. A heat exchanger is preheated to provide stagnation temperatures up to 660° F and the stagnation pressure can be varied from 60 to 200 psia. Additional details on this tunnel are presented in reference 1.

Panel holder and mounting arrangement.- The panels were mounted in a panel holder which extended vertically through the test section (fig. 2). A cross section of the panel holder is shown in figure 3. As can be seen from figure 3, the panel holder has a half-wedge leading edge, flat sides, and a recess

29 inches wide, 30 inches high, and 5 inches deep for accommodating test specimens; the installation of instrumentation in the cavity reduces the effective depth to approximately 3.5 inches. The recess is located on the nonbeveled side of the panel holder. Pneumatically operated sliding doors protect test specimens from aerodynamic buffeting and heating during tunnel starting and shutdown. Aerodynamic fences prevent shock waves emanating from the doors from interfering with the airflow over the test specimen. (The flow conditions over the exposed surface of a flat panel are essentially free-stream conditions as determined from pressure surveys of a flat calibration panel (ref. 1).) A vent-door arrangement on the side opposite the recess for the panel is used to control the pressure inside the cavity behind the test specimen (fig. 3).

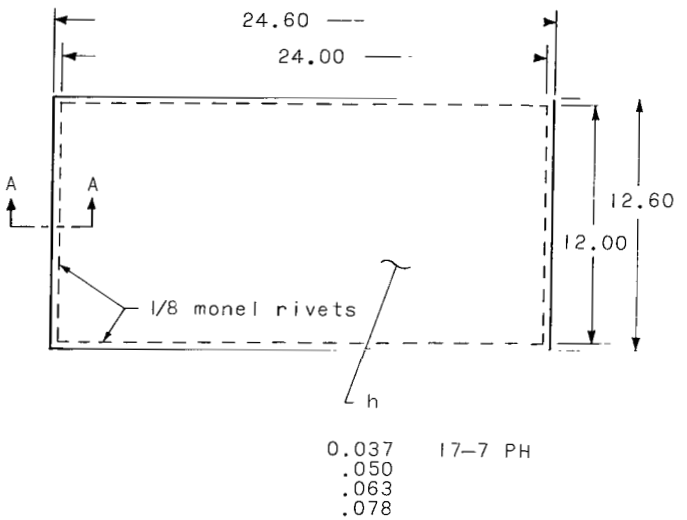

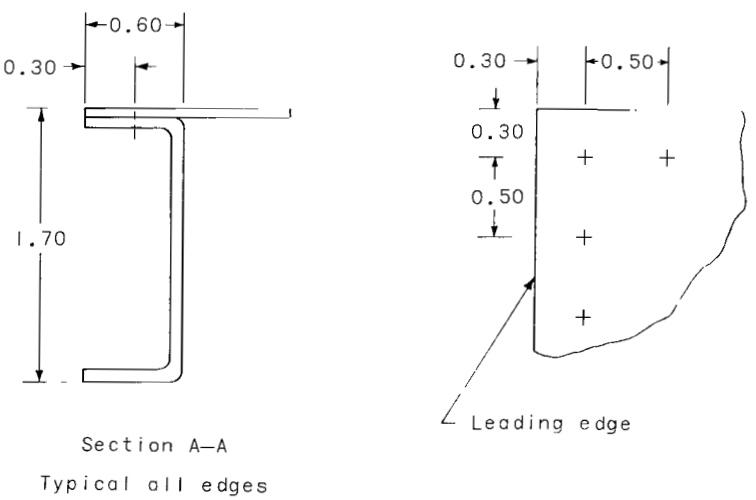

Figure 1.- Panel construction details. (All dimensions are in inches.)

All panels were mounted flush with the flat surface of the panel holder. The panels were attached to a mounting plate which was attached to a mounting fixture which in turn was bolted to a panel holder (fig. 4). Such a mounting arrangement provided elastic restraint against both inplane and rotational displacements at the edges of the panel. To improve control of the differential pressure, all openings to the cavity behind the panel, except the vent door, were sealed.

Instrumentation

Iron-constantan thermocouples, spotwelded to the panels at the 21 locations shown by the diamonds in figure 5, were used to measure panel temperatures. Variable-reluctance-type deflectometers were used to determine motion of the panel skin. The deflectometers were located approximately one-quarter inch behind the panel at the 6 positions indicated by the circles in figure 5. In addition, high-speed 16-millimeter motion pictures provided supplementary data on panel behavior. Grid lines were painted on panel skins for photographic purposes.

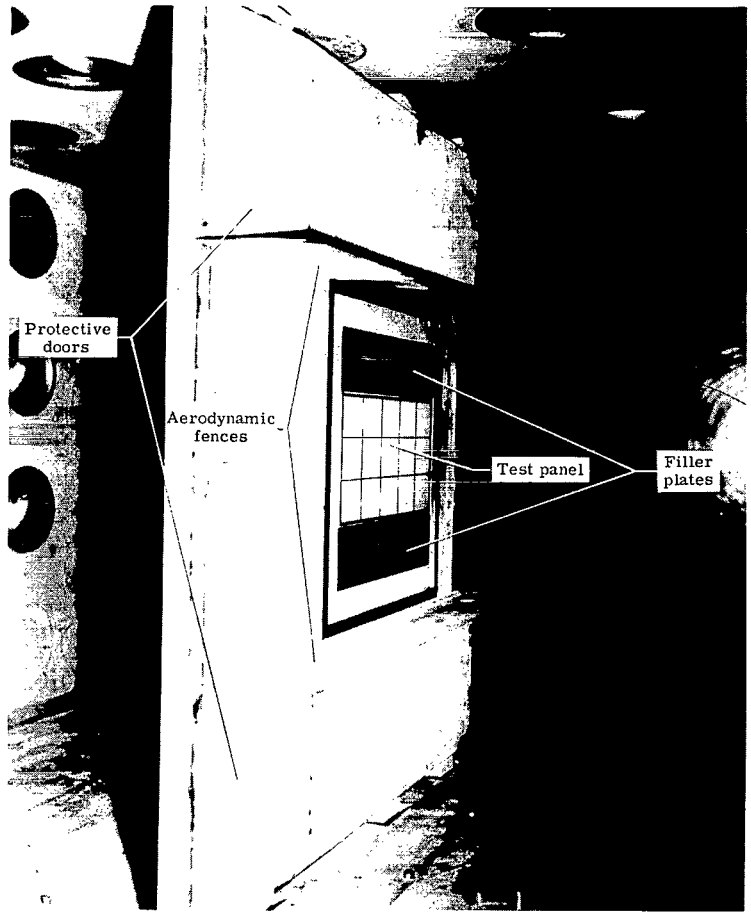

L-62-843.1

Figure 2.- Panel mounted in panel holder as viewed from upstream. Panel holder doors are in open position.

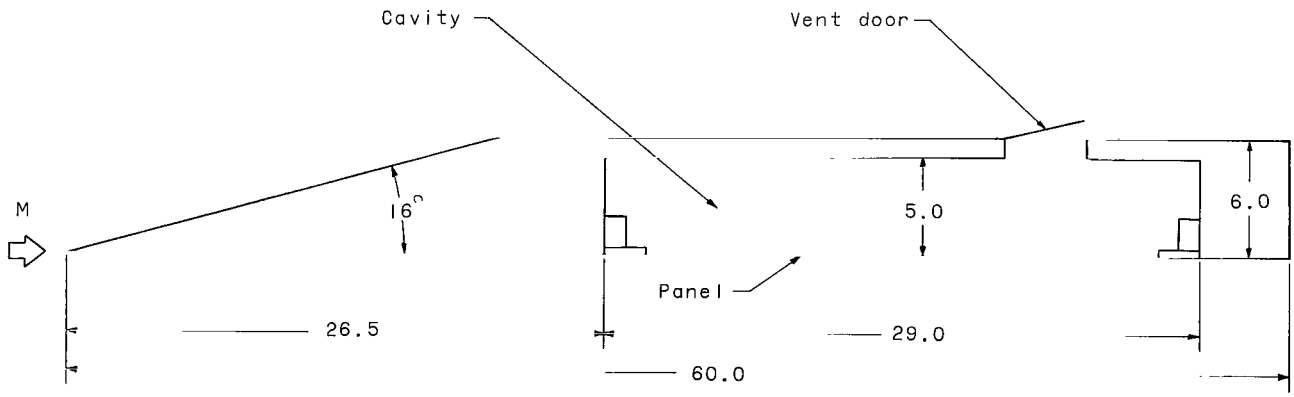

Figure 3.- Cross section of panel holder. (All dimensions are in inches.)

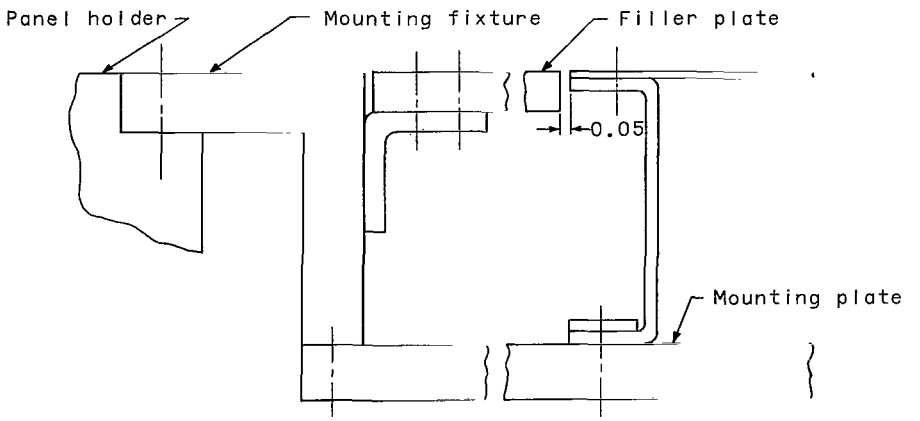

(a) Longitudinal edges.

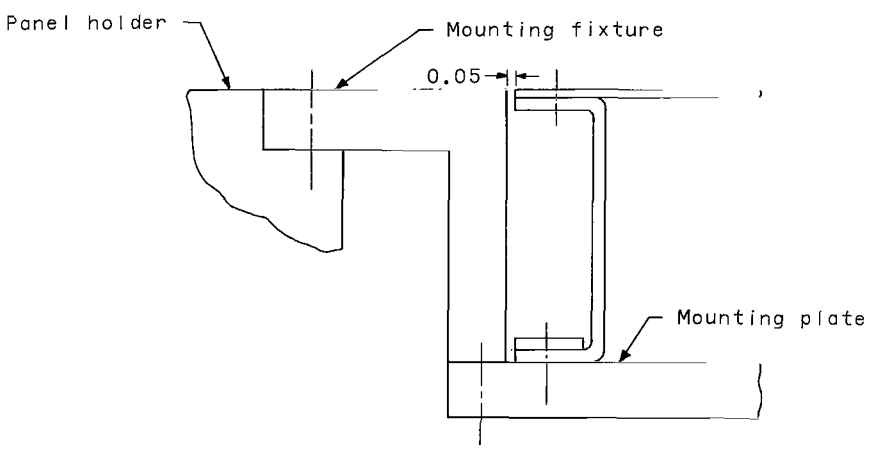

(b) Leading and trailing edges.

Figure 4.- Panel mounting detail.

Quick-response, strain-gage-type pressure transducers were used to measure static pressures at various locations on the panel holder and in the cavity behind the panels. Tunnel stagnation pressures were obtained from static pressures measured in the tunnel settling chamber. Stagnation temperatures were measured by total temperature probes located in the test section. For each test all temperature and pressure data were recorded on magnetic tape. Deflectometer data and differential pressures were recorded on high-speed oscillographs.

Test Procedure

The tests were conducted at a Mach number of 3.0, at dynamic pressures from 1,500 to 5,000 pounds per square foot, and at stagnation temperatures from 310° F to 650° F. The protective doors on the panel holder were opened after the

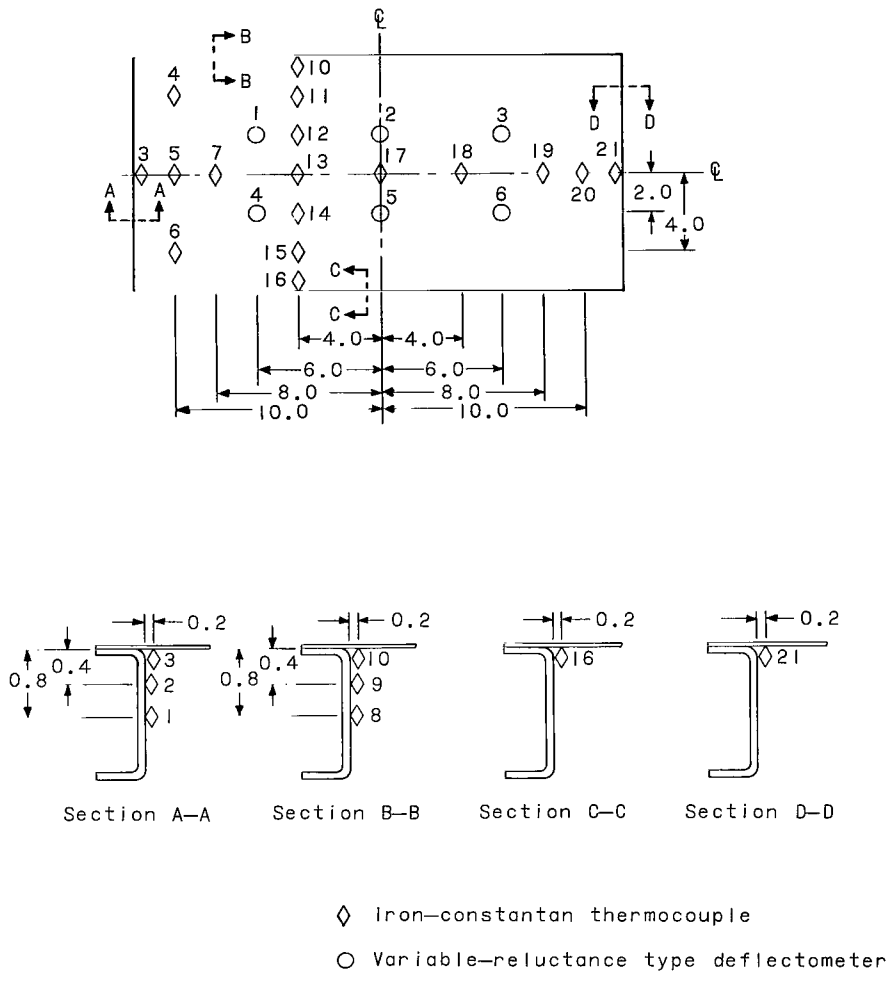

Figure 5.- Location of panel instrumentation.

desired test conditions were established and were closed 3 seconds prior to tunnel shutdown. The duration of test conditions varied between approximately 10 and 60 seconds. The stagnation temperature was essentially constant during most tests but decreased during the latter portions of some tests. The dynamic pressure was constant during the first few seconds of all tests but was varied during the remainder of most tests in an attempt to obtain as many flutter points as possible; the occurrence of flutter was determined by monitoring the high-speed oscillographs during a test. The usual procedure for varying the dynamic pressure was as follows:

(a) If no flutter had occurred after a predetermined period of time, the dynamic pressure was increased in an attempt to initiate flutter

(b) If flutter had started and stopped, the dynamic pressure was increased in an attempt to restart flutter

(c) If the panel was still fluttering after a predetermined period of time, the dynamic pressure was decreased in an attempt to stop flutter.

The differential pressure Δp was controlled manually during the tests. During the earlier tests Δp was to be maintained near zero. However, inaccurate control resulted in large negative values of Δp. Accurate control of Δp was obtained during the second test series. For these tests Δp was usually maintained near zero but was intentionally varied during several tests.

RESULTS AND DISCUSSION

Flutter was obtained in 19 of the 20 tests made in this investigation. Flutter occurred for both thermally stressed but unbuckled panels and for thermally buckled panels. Pertinent data for all tests are given in table I. The data tabulated include the stagnation temperature T_t, dynamic pressure q, panel skin temperature increase ΔT, differential pressure Δp, flutter parameter $\left(\frac{q}{\beta E}\right)^{1/3}\frac{a}{h}$, temperature parameter $\alpha\,\Delta T\left(\frac{a}{h}\right)^2$, and flutter frequency f.

Panel Temperatures

At the beginning of a test the panel skin and supporting structure were at nearly the same temperature. Any temperature increase of the panels prior to opening the protective doors was usually insignificant. After a panel was exposed to the airstream, the skin temperature increased in a manner similar to the typical temperature histories shown in figure 6 (test 3). The top curve represents the average of thermocouples 7, 12, 13, 14, 17, 18, and 19; individual temperatures for these thermocouples were within 10° F of the average value. The temperature histories for thermocouples 1 to 6, 8 to 11, 15, 16, 20, and 21 indicate that there were appreciable lateral and longitudinal temperature gradients in the panel skin near the supporting structure and large temperature gradients in the supporting structure. However, these temperature variations were neglected in analyzing the test data, and the average increase in temperature of thermocouples 7, 12, 13, 14, 17, 18, and 19 was considered to be the temperature increase ΔT of the panel skin.

Flutter Parameters

The flutter data obtained in this investigation are summarized in terms of a dimensionless flutter parameter and a dimensionless temperature parameter. Of the quantities in the flutter parameter $\left(\frac{q}{\beta E}\right)^{1/3}\frac{a}{h}$, which is proportional to the cube root of the primary panel flutter parameter given by theory (for example, in ref. 6), only the dynamic pressure q and the skin thickness h were varied in this investigation. Because of the short duration of the tests, changes in material properties with temperature were assumed to be negligible.

TABLE I.- PANEL FLUTTER DATA

$$\left[E = 29.5 \times 10^6 \text{ psi}, \quad \alpha = 6.1 \times 10^{-6} \frac{\text{in./in.}}{^\circ F}\right]$$

Test	h, in.	T_t, °F	q, psf	ΔT, °F	Δp, psi	$\left(\frac{q}{\beta E}\right)^{1/3} \frac{a}{h}$	$\alpha \Delta T \left(\frac{a}{h}\right)^2$	f, cps	Flutter start or stop	Panel condition[1]	Type of motion[2]
1	0.037	400	2460	95	-0.02	3.82	244	65	Start	F	T
2	.037	395	2840	9	.15	3.98	23	72	Start	F	S
3	.037	320	3200	36	-.15	4.17	92	71	Start	F	T
			3100	62	-.55	4.13	159	69	Stop	F	T
			2370	81	-.38	3.77	208	61	Start	F	T
			2160	94	-.41	3.66	241	---	Stop	F	T
			1840	104	-.34	3.47	267	58	Start	F	T
			1520	111	-.37	3.26	285	---	Stop	F	T
4	.037	585	1755	135	-.18	3.41	346	51	Start	F	T
			1755	170	-.19	3.41	436	---	Stop	B	T
			4690	323	-.30	4.74	829	65	Start	B	T
5	.037	450	1725	7	-.09	3.39	18	68	Start	F	S
			1695	66	-.35	3.37	169	60	Stop	F	S,T
			1695	76	-.34	3.37	195	---	Start	F	T
6	.037	355	2730	102	-.33	3.96	262	65	Start	F	T
7	.037	330	3460	75	-.29	4.28	192	65	Start	F	T
			1510	129	-.26	3.25	331	55	Stop	B	T
8	.037	310	3250	6	-.12	4.19	15	80	Start	F	S
9	.037	645	2790	78	-.31	3.98	200	69	Start	F	T
10	.037	350	2020	12	.01	3.58	31	73	Start	F	S
11	.050	570	4400	238	-.69	3.43	334	73	Start	F	T
			4400	245	-.41	3.43	344	73	Stop	B	T
12	.050	625	3000	178	-.16	3.02	250	70	Start	F	T
			3000	201	-.16	3.02	282	70	Stop	B	T
13	.050	500	3220	21	-.26	3.09	30	70	Start	F	S
14	.050	495	2730	42	-.07	2.92	59	71	Start	F	S
			2730	264	-.28	2.92	371	---	Stop	B	T
			2910	271	-.34	2.99	381	70	Start	B	T
15	.050	580	2455	65	-.05	2.82	91	75	Start	F	S
			1500	181	-.15	2.40	254	73	Stop	F	S,T
			1810	201	-.27	2.55	282	67	Start	F	T
16	.050	540	2480	44	.01	2.83	61	70	Start	F	S
17	.050	500	3850	20	.05	3.28	28	75	Start	F	S
			3850	65	-.08	3.28	91	70	Stop	F	S,T
			4890	211	-.11	3.55	297	70	Start	F	T
			1780	233	-.25	2.54	327	52	Stop	B	T
18	.063	540	3110	115	.05	2.43	102	82	Start	F	S
			1605	246	.01	1.95	218	85	Stop	B	S
19	.063	650	1495	147	-.03	1.90	138	---	-----	F-B	N
			4450	360	-.04	2.73	319	---	Start	B	S
			4425	375	-.09	2.73	332	---	Stop	B	S
20	.078	645	3825	239	-.05	2.10	138	---	-----	F-B	N

[1] F flat
B buckled

[2] S standing-wave flutter
T traveling-wave flutter
S,T combination of standing-wave and traveling-wave motion
N no flutter

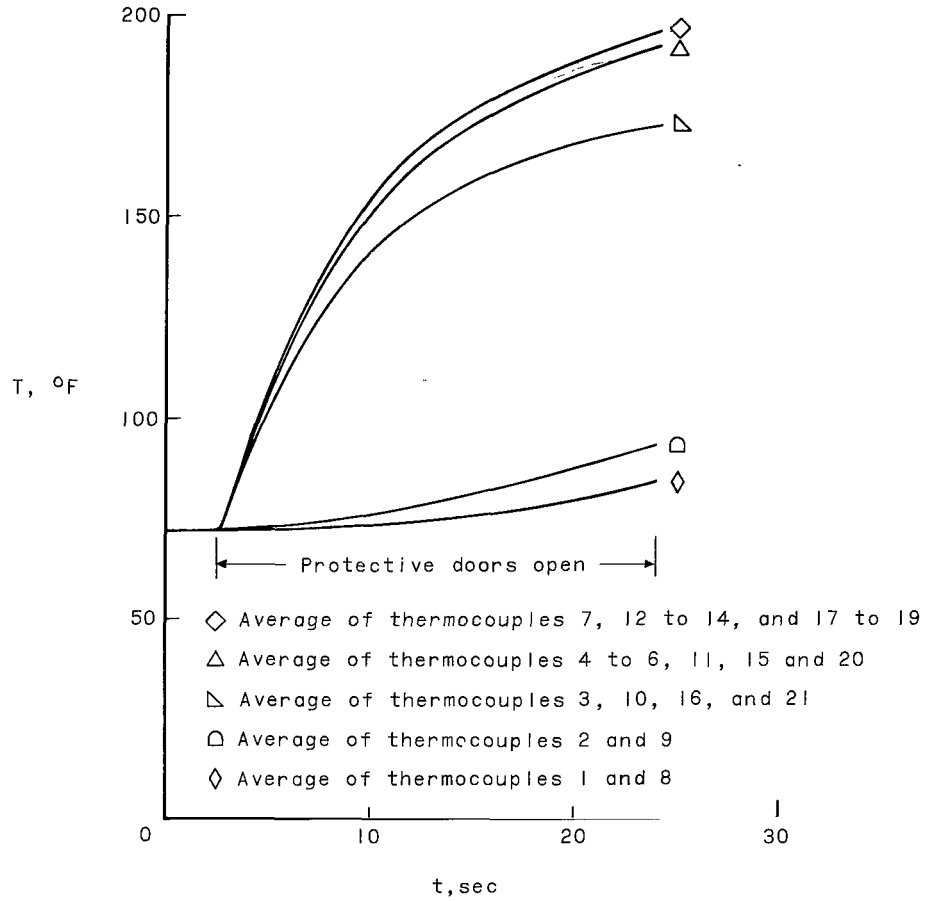

Figure 6.- Measured panel temperatures for test 3.

The temperature parameter $\alpha\,\Delta T\left(\frac{a}{h}\right)^2$ is a measure of the thermally induced midplane compressive stress in the skin in terms of the temperature rise ΔT, which has been nondimensionalized so as to be proportional (for no edge displacements) to the stress ratio $\frac{N_x a^2}{\pi^2 D}$; the ratio $\frac{N_x a^2}{\pi^2 D}$ is frequently used in theoretical analyses (for example, ref. 6). The temperature parameter was not modified to account for the effects of Δp as was done approximately in reference 2. Preference for the unmodified parameter resulted from several considerations. The panels of the present investigation were elastically restrained in such a manner that both inplane and rotational displacements occurred at the edges as the panel was heated. The inplane and rotational displacements were coupled and the rotation associated with inplane displacements due to heating induced curvature of the panel skin, with the amount of curvature (for $\Delta p = 0$) depending on the magnitude of ΔT. Therefore, the effects of Δp on the midplane stress and deflection shape would depend on the direction and magnitude of the pressure loading and the magnitude of ΔT. Because of these complications, modification

of the temperature parameter to account for the effects of Δp was not considered feasible in this investigation.

Flutter Results

Results from all tests are presented in figure 7 in terms of the flutter parameter and the temperature parameter. For many tests the pressure difference across the panels was large $\left(|\Delta p| > 0.15 \text{ psi}\right)$ and negative, and flutter occurred

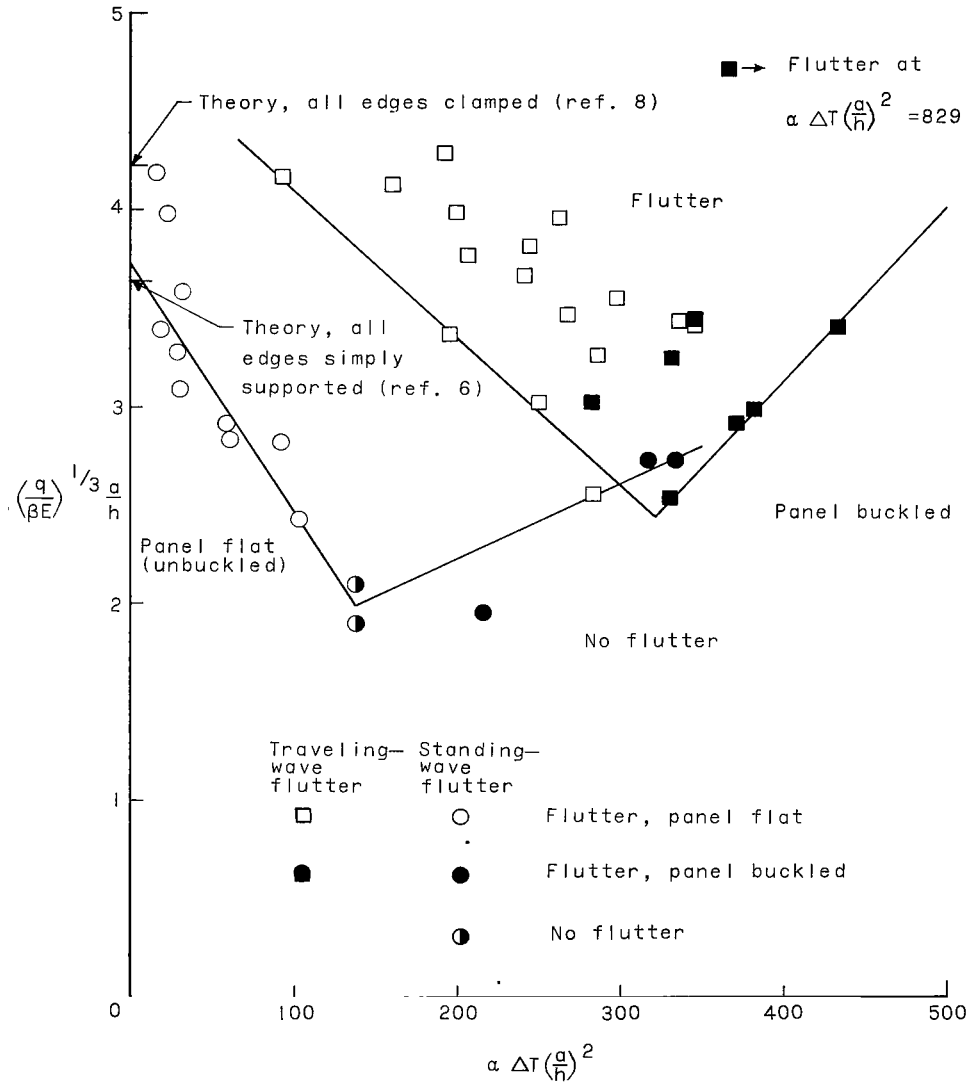

Figure 7.- Effects of differential pressure, thermal stress, and buckling on flutter characteristics of elastically restrained panels with length-width ratios of 2.

as a traveling-wave type of motion that was periodic but not necessarily harmonic. The square symbols in figure 7 represent flutter start or stop for this type of motion. The open symbols apply to panels that were not thermally buckled when dynamically stable and the solid symbols pertain to panels in a thermally buckled condition when dynamically stable. More precise control of the pressure difference $\left(|\Delta p| < 0.10 \text{ psi}\right)$ disclosed a standing-wave type of flutter that was harmonic. The circular symbols represent flutter points for this type of motion. Again, an open symbol indicates that a panel was not thermally buckled and a solid symbol indicates that a panel was thermally buckled. The half-solid symbols are no-flutter points. The solid curves are boundaries arbitrarily faired through the experimental flutter points.

As can be seen from figure 7, there are two distinct boundaries, one associated with standing-wave flutter and one with traveling-wave flutter. Each boundary consists of an unbuckled-panel portion, a buckled-panel portion, and a transition point, at the intersection of the two portions, where a panel is most susceptible to flutter. The overall trends exhibited by both boundaries are similar to trends obtained in previous experimental investigations (refs. 1 to 5).

Traveling-wave flutter.- As can be seen from table I, most traveling-wave flutter occurred when the differential pressure was large $\left(|\Delta p| > 0.15 \text{ psi}\right)$ and negative. However, for tests 1 and 17, traveling-wave flutter occurred for $|\Delta p| < 0.15$ psi. For a given value of $\left(\frac{q}{\beta E}\right)^{1/3}\frac{a}{h}$, the temperature increase required for traveling-wave flutter was much larger than the increase required for standing-wave flutter. As can be seen from figure 7, there is considerable scatter in the traveling-wave flutter data. This scatter is considered to be due to the large variations in Δp (-0.02 to -0.69 psi) for the traveling-wave flutter. Neither the flutter parameter nor the temperature parameter account for the effects of Δp and no attempt was made to account for the effects of Δp on either the deflection shape or midplane stress. The boundary was not extended back to $\alpha \Delta T\left(\frac{a}{h}\right)^2$ of zero as this value would not indicate zero midplane stress for large values of Δp. However, the traveling-wave flutter boundary indicates that the thickness required to prevent flutter of a panel on the verge of buckling is considerably larger than the thickness required for panels subjected to only small amounts of midplane compressive stress.

The flutter mode had three half-waves in the longitudinal (streamwise) direction and one half-wave in the lateral direction and was similar (as to the number of half-waves) to the buckling mode. The similarity in flutter and buckling modes has been observed in previous investigations (refs. 1 to 4). The flutter motion consisted of a low frequency oscillation with some higher-frequency lower-amplitude motion present (fig. 8). As can be seen from figure 8, the low frequency motion at the three deflectometer locations was slightly out of phase.

One panel was damaged during traveling-wave flutter. Observation of the test panel at the end of test 4 revealed that fatigue cracks had developed along the rivet lines at the trailing edge and the extreme downstream portions of the

longitudinal edges. This panel had been subjected to 7.9 seconds of flutter during test 3 and 30.6 seconds of flutter during test 4.

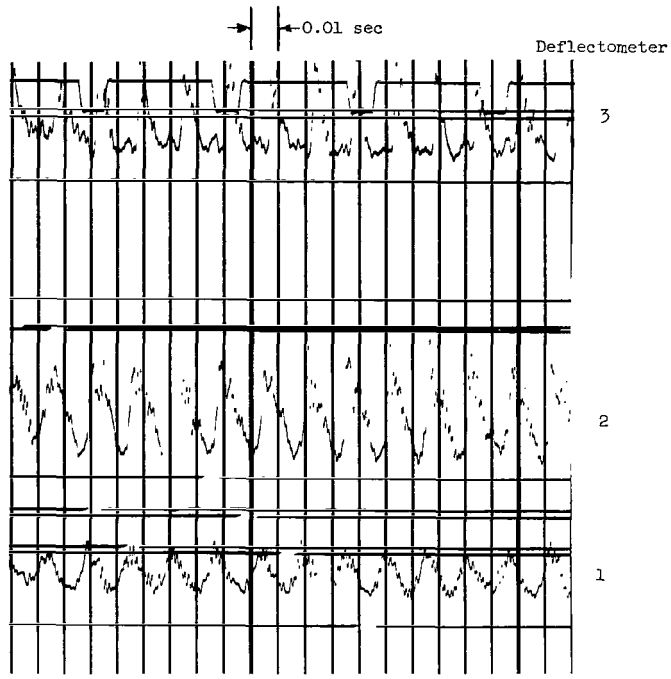

Figure 8.- Sample deflectomer record showing traveling-wave flutter.

Standing-wave flutter.- As can be seen from table I, most standing-wave flutter occurred when Δp was small ($\Delta p < 0.10$ psi). However, for tests 2, 8, and 13, Δp exceeded 0.10 psi with a maximum value of Δp of -0.26 psi occurring in test 13. If these data are excluded, there is little scatter in the standing-wave flutter data, suggesting that the parameter $\alpha \Delta T\left(\frac{a}{h}\right)^2$ provides good correlation of flutter data for heated panels when Δp is small. The arbitrary boundary faired through the standing-wave flutter data (fig. 7) indicates a value of $\left(\frac{q}{\beta E}\right)^{1/3} \frac{a}{h}$ of 3.75 for $\alpha \Delta T\left(\frac{a}{h}\right)^2$ of zero. However, the overall scatter is such that the value of $\left(\frac{q}{\beta E}\right)^{1/3} \frac{a}{h}$ for $\alpha \Delta T\left(\frac{a}{h}\right)^2$ of zero could possibly be between 3.45 and 4.45. The boundary shown in figure 7 indicates that at the transition point $\left(\frac{q}{\beta E}\right)^{1/3} \frac{a}{h}$ is approximately 2.0; the flutter and no-flutter points obtained in the vicinity of $\left(\frac{q}{\beta E}\right)^{1/3} \frac{a}{h} = 2.0$ suggest this value is essentially correct for the transition point. Thus, the thickness required to prevent flutter when a panel is on the verge of buckling (transition point) is approximately twice the thickness required to prevent flutter of an unheated panel.

The flutter mode consisted of one half-wave in both the lateral and longitudinal directions and again appeared to be similar to the buckle pattern. Motion pictures and deflectometer data revealed that the maximum amplitude of motion occurred in the downstream half of the panel and that the motion was essentially in phase at all three deflectometer locations (fig. 9). As can be seen from figure 9, the variations in amplitude at the three deflectometer stations are larger than the variations for traveling-wave flutter (fig. 8). No apparent damage to the panels occurred during standing-wave flutter.

Effects of differential pressure.- The results presented in table I and figure 7 indicate that the flutter behavior was dependent on the magnitude and

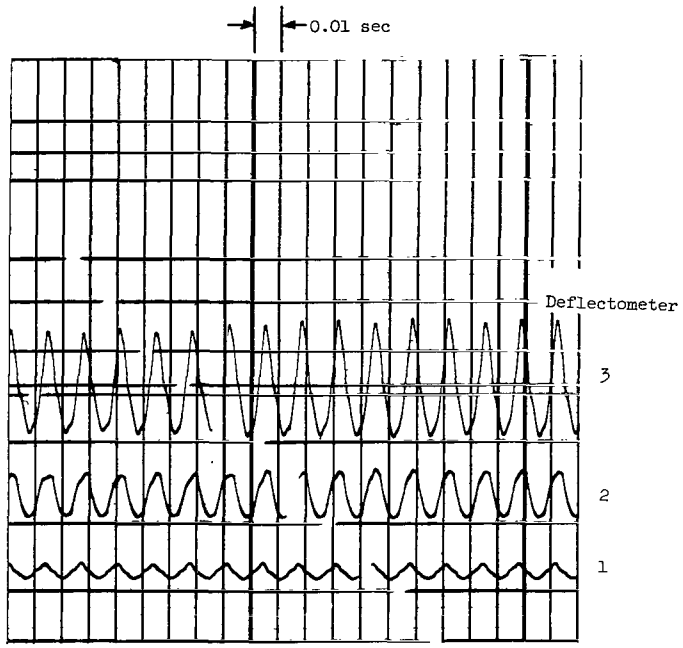

Figure 9.- Sample deflectomer record showing standing-wave flutter.

possibly the direction of the pressure difference across the panel. For example, in several instances a panel was observed to respond to the standing-wave flutter boundary during one test and the traveling-wave flutter boundary during another test. Consider tests 8 and 9 (table I), which were conducted on the same panel. During test 8, Δp was small and standing-wave flutter occurred. However, during test 9, Δp was large (and negative), standing-wave flutter was suppressed, and traveling-wave flutter occurred at a ΔT much larger than indicated by the standing-wave boundary. This result clearly indicates that the type of flutter (resulting from an increase in ΔT) was dependent on the magnitude of the differential pressure. This is indicated also by the results of test 5 which are shown in figure 10. Figure 10(a) shows the variation of Δp with $\alpha \Delta T\left(\frac{a}{h}\right)^2$ and figure 10(b) shows the variation of $\left(\frac{q}{\beta E}\right)^{1/3} \frac{a}{h}$ with $\alpha \Delta T\left(\frac{a}{h}\right)^2$. Figure 10(b) also shows the flutter boundaries of figure 7. The circular symbol shows the start of standing-wave flutter $\left(\alpha \Delta T\left(\frac{a}{h}\right)^2 = 18, \quad \Delta p = -0.09 \text{ psi}\right)$. The differential pressure remained essentially constant until $\alpha \Delta T\left(\frac{a}{h}\right)^2$ reached 110. As $\alpha \Delta T\left(\frac{a}{h}\right)^2$ increased beyond 110, Δp began to increase negatively and the standing-wave motion changed to a combination of standing-wave motion and traveling-wave motion but was not distinctly either type. This composite motion stopped when $\alpha \Delta T\left(\frac{a}{h}\right)^2$ reached 169 and Δp was -0.35 psi. As $\alpha \Delta T\left(\frac{a}{h}\right)^2$ increased beyond 169, Δp was again nearly constant. When $\alpha \Delta T\left(\frac{a}{h}\right)^2$ reached 195 (Δp = -0.34 psi) traveling-wave flutter started, as indicated by the square symbol, and continued to the end of the test; Δp was approximately -0.35 to -0.30 psi during the remainder of the test. The cessation of standing-wave flutter due to an increasing negative Δp also occurred during tests 15 and 17; for clarity these flutter points are omitted in figure 7.

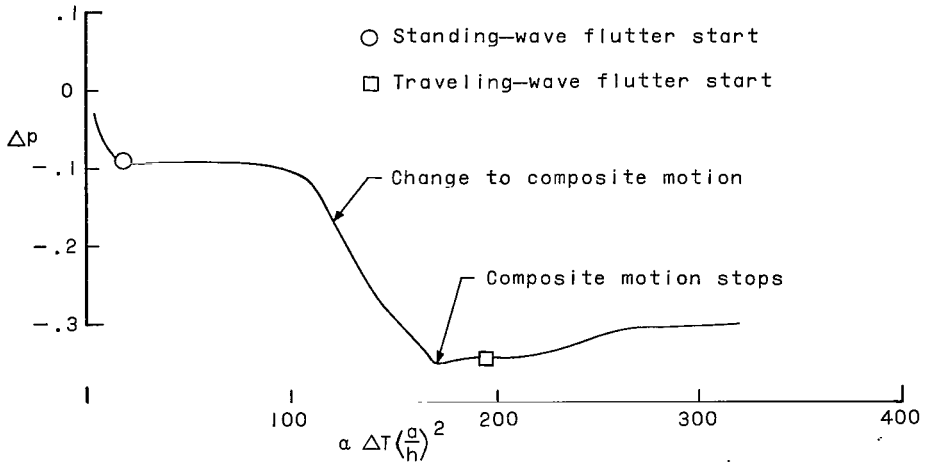

(a) Differential pressure.

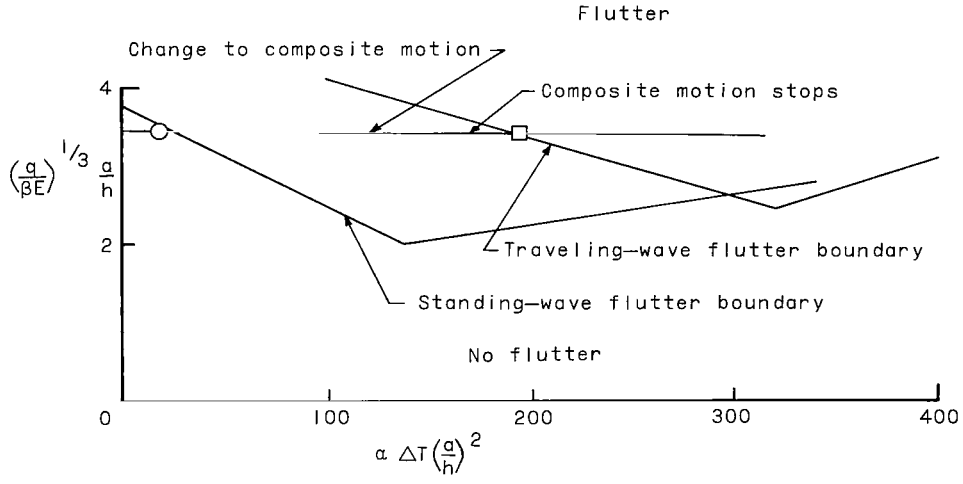

(b) Flutter parameter.

Figure 10.- Variation of flutter parameter and differential pressure with temperature parameter during test 5 wherein both standing-wave and traveling-wave flutter occurred.

It is interesting to note that Δp was negative for all traveling-wave flutter. As noted previously, the panel edge restraint was such that the heated panels could be considered as slightly curved panels (bowed into the airflow). A negative pressure loading on such a panel could possibly change the deflection shape from a single half-wave to several half-waves. On the other hand, a positive pressure loading would not be expected to change the number of half-waves of the deflection shape. This suggests the possibility that the occurrence of the traveling-wave flutter depended on not only the magnitude of Δp but also on the direction of loading. Indeed, for test 2, Δp was fairly large and positive ($\Delta p = 0.15$ psi) but standing-wave flutter occurred. However, the lack of flutter

data for large positive values of Δp precludes any definite conclusions concerning the effect of the direction of loading.

The reasons for the observed flutter behavior are not completely understood, nor is it clear whether the effects of Δp result from aerodynamics (change in deflection shape), variations in midplane stress, or both. However, the results suggest that the variations in flutter behavior were due to the type of panel edge restraint and variations in the magnitude and possibly the direction of Δp.

Comparison With Theory

The panels of this investigation were partially restrained on all edges. Such edge restraint is generally assumed to be intermediate between simply supported and fully clamped; hence, the experimental results will be compared with theory for these two limiting cases. Since the experimental data are presented in terms of temperatures rather than measured stresses, the experimental results will be compared with theory only for the condition of zero midplane stress $\left(\alpha \Delta T\left(\frac{a}{h}\right)^2 = 0\right)$.

Theoretical predictions for zero midplane stress were calculated from the "exact" solutions of the flutter equation obtained by Hedgepeth (all edges simply supported, ref. (6)) and Houbolt (all edges clamped, ref. (8)). It should be noted that the solution for clamped panels is based on an assumed deflection shape in the lateral direction. In addition, in the theoretical value for clamped edges the Mach number M, which appears in the parameter $\frac{2qa^3}{MD}$ was replaced by β where $\beta = \sqrt{M^2 - 1}$. As can be seen from figure 7, for $\alpha \Delta T\left(\frac{a}{h}\right)^2 = 0$ the standing-wave flutter boundary is bracketed by the theoretical values of $\left(\frac{q}{\beta E}\right)^{1/3} \frac{a}{h}$ of 3.64 (all edges simply supported) and 4.23 (all edges clamped). Considering the overall scatter in the data the experimental results of this investigation appear to be in reasonable agreement with either theory for zero stress.

The experimental results at the transition point could be compared with theoretical values obtained from the transtability concept introduced by Isaacs (ref. 12). However, the stress ratio σ_y/σ_x and edge restraint for the panels of this investigation are not known accurately and the results of reference 3 indicate that the flutter characteristics of panels on the verge of buckling are very sensitive to both the stress ratio σ_y/σ_x and the edge restraint. Thus, the experimental results at the transition point are not compared with theory as the resulting agreement would depend to a large extent on the assumptions for σ_y/σ_x and the panel edge conditions.

CONCLUSIONS

Flat, single-bay, skin-stiffener panels with length-width ratios of 2 were tested in the Langley 9- by 6-foot thermal structures tunnel to determine some of the effects of thermal stress and buckling on the flutter characteristics of elastically restrained panels. The tests were conducted at a Mach number of 3.0 and at various dynamic pressures, stagnation temperatures, and differential pressures. The tests revealed the following:

1. Two distinct flutter boundaries were obtained for two different types of flutter, standing-wave flutter and traveling-wave flutter. The standing-wave flutter mode consisted of one half-wave in both the lateral and longitudinal directions, whereas the traveling-wave flutter mode had three half-waves in the longitudinal (streamwise) direction.

2. Standing-wave flutter usually occurred when the differential pressure was less than 0.10 psi. Traveling-wave flutter generally occurred when the differential pressure was greater than 0.15 psi and when the direction of loading was toward the cavity behind the panel. In several instances the initial flutter was of the standing-wave type, but increases in the differential pressure suppressed this motion and eventually initiated traveling-wave flutter.

3. The flutter trends indicated by both boundaries were similar to experimental trends obtained previously for thermally stressed panels with length-width ratios from 0.96 to 10.

4. For both types of flutter, the thickness required to prevent flutter of a panel on the verge of buckling (transition point) was considerably larger than the thickness required to prevent flutter of a panel subjected to only small amounts of midplane compressive stress.

5. For the condition of zero midplane stress, the experimental results for standing-wave flutter were in general agreement with theoretical results.

Langley Research Center,
National Aeronautics and Space Administration,
Langley Station, Hampton, Va., September 6, 1963.

REFERENCES

1. Dixon, Sidney C., Griffith, George E., and Bohon, Herman L.: Experimental Investigation at Mach Number 3.0 of the Effects of Thermal Stress and Buckling on the Flutter of Four-Bay Aluminum Alloy Panels With Length-Width Ratios of 10. NASA TN D-921, 1961.

2. Dixon, Sidney C.: Experimental Investigation at Mach Number 3.0 of Effects of Thermal Stress and Buckling on Flutter Characteristics of Flat Single-Bay Panels of Length-Width Ratio 0.96. NASA TN D-1485, 1962.

3. Dixon, Sidney C.: Application of Transtability Concept to Flutter of Finite Panels and Experimental Results. NASA TN D-1948, 1963.

4. Guy, Lawrence D., and Bohon, Herman L.: Flutter of Aerodynamically Heated Aluminum-Alloy and Stainless-Steel Panels With Length-Width Ratio of 10 at Mach Number of 3.0. NASA TN D-1353, 1962.

5. Bohon, Herman L.: Panel Flutter Tests on Full-Scale X-15 Lower Vertical Stabilizer at Mach Number of 3.0. NASA TN D-1385, 1962.

6. Hedgepeth, John M.: Flutter of Rectangular Simply Supported Panels at High Supersonic Speeds. Jour. Aero. Sci., vol. 24, no. 8., Aug. 1957, pp. 563-573, 586.

7. Movchan, A. A.: On the Stability of a Panel Moving in a Gas. NASA RE 11-21-58W, 1959.

8. Houbolt, John C.: A Study of Several Aerothermoelastic Problems of Aircraft Structures in High-Speed Flight. Nr. 5, Mitteilungen aus dem Institut für Flugzeugstatik und Leichtbau. Leemann (Zürich), c.1958.

9. Fralich, Robert W.: Postbuckling Effects on the Flutter of Simply Supported Rectangular Panels at Supersonic Speeds. NASA TN D-1615, 1963.

10. Kobayashi, Shigeo: Flutter of Simply Supported Rectangular Panels in a Supersonic Flow. Reprinted from Trans. of Japan Soc. for Aero. and Space Sci., vol. 5, no. 8, 1962, pp. 79-89.

11. Guy, Lawrence D., and Dixon, Sidney C.: A Critical Review of Experiment and Theory for Flutter of Aerodynamically Heated Panels. Symposium on Dynamics of Manned Lifting Planetary Entry, S. M. Scala, A. C. Harrison, and M. Rodgers, eds., John Wiley & Sons, Inc., c.1963, pp. 568-595.

12. Isaacs, R. P.: Transtability Flutter of Supersonic Aircraft Panels. U.S. Air Force Project RAND P-101, The RAND Corp., July 1, 1949.

NASA-Langley, 1963 L-3520